Interaction between Polymer Brush and Nanoparticle: Brownian Dynamics Investigation

Q.Y. Zhang* and X. Xiang
Department of Mathematics and Physics, Chongqing University of Science and Technology
Chongqing, 401331, China

(Received October 2, 2012; in final form February 22, 2013)

We use Brownian dynamics simulations to study the adsorption behavior of a nanosized particle on polymer brushes. The adsorption process, the dynamic behavior of the nanoparticle in brush, the penetration depth, and the diffusion coefficient of the nanoparticle in different depths of the brush are all investigated for different grafting densities. We provide an area density Γ, which is the area average of the monomer number above the embedded nanoparticle in brush. We find that this area density explains well qualitatively the experimental phenomenon that the nanoparticles exhibit a maximum in the adsorbed amount as a function of the grafting density of brush.

DOI: 10.12693/APhysPolA.123.642
PACS: 05.45.Xt, 05.45.Jn

1. Introduction

The interaction of nanoparticles with polymer brushes is an area which has received considerable theoretical and experimental considerations [1–7], because of their important theoretical significances and technological applications such as the colloidal stabilization and lubrication [8, 9], nanoparticle formation at the polymer brush/air interface [1, 10, 11], and cell adhesion [12–14] in biological sciences. Polymer brushes, formed by densely grafting polymers to a substrate, produce a steric repulsion when deformed, which offers effective means of countering van der Waals interactions. Brushes now provide a convenient method of stabilizing colloidal suspensions [15, 16], and are being investigated as a way of preventing adsorption on surfaces by nanoparticles and macromolecules such as proteins [17, 18].

Experiments show that with the increase of the grafting density of brush, the amount of the adsorption nanoparticles on brush has a maximal value [19]. High grafting density means more adsorption monomers, correspondingly, the steric repulsions between monomers are strong and the nanoparticle cannot penetrate deep. While low grafting density leads to less adsorption monomers, the corresponding weak steric repulsions allow the nanoparticle to penetrate deep. We find the area density Γ, which is defined by the area average of the monomer number above the embedded nanoparticle in brush, can provide a useful guide for the understanding of the dependence of adsorption amount on grafting density. For a large particle, the adsorption on brush will squeeze the polymer chains. So, the detailed polymer chain structures around the sink nanoparticle are also interesting.

*corresponding author; e-mail: qyzhang520@163.com

In the present paper, we will investigate the simple case of single nanoparticle adsorption on brush. The adsorption process, penetration depth, the dynamic behavior as well as the diffusion coefficient of nanoparticle in brush, are all investigated for different grafting densities.

2. Model and simulation details

Following the previous Brownian dynamics studies of polymers [20–23], polymer chains are modeled using the Grest–Kremer bead-spring model [24]. The interaction potential between polymer–substrate, monomer–monomer and particle–substrate has been chosen as purely repulsive Lennard–Jones (LJ) potential

$$U_{\mathrm{LJ}}(r) = 4\epsilon_{\mathrm{mm}}\left[\left(\frac{\sigma_{\mathrm{mm}}}{r}\right)^{12} - \left(\frac{\sigma_{\mathrm{mm}}}{r}\right)^{6} + \frac{1}{4}\right] \tag{1}$$

for $r \leq 2^{1/6}\sigma_{\mathrm{mm}}$ and 0 otherwise. ϵ_{mm} denotes the interaction strength. We set $\sigma_{\mathrm{mm}} = 1.0$ and $\epsilon_{\mathrm{mm}} = 1.0$, as units of length and energy correspondingly. For polymer–substrate interaction, only the z component is considered in r.

The spring potential of our bead-spring model is created by adding a finitely extensible nonlinear elastic (FENE) potential [25]:

$$U_{nn}(r) = -\frac{1}{2}k_{\mathrm{b}}b_{\max}^2 \ln\left(1 - \left(\frac{r}{b_{\max}}\right)^2\right), \quad r < b_{\max}, \tag{2}$$

where r is the length of a bond, $b_{\max}$ is the maximum bond extension, and k_{b} is the spring constant. We choose the constants $b_{\max} = 1.5\sigma_{\mathrm{mm}}$ and $k_{\mathrm{b}} = 30\epsilon_{\mathrm{mm}}/\sigma_{\mathrm{mm}}^2$ as usually done [26].

For the interaction between nanoparticle and polymer monomers, we use the standard Lennard–Jones form,

$$U_{\text{m-np}}(r) = 4\epsilon_{\text{m-np}}\left[\left(\frac{\sigma_{\text{m-np}}}{r - R_0}\right)^{12} - \left(\frac{\sigma_{\text{m-np}}}{r - R_0}\right)^{6} + \frac{1}{4}\right]. \tag{3}$$

We should keep in mind that the r here is the distance between the center of the nanoparticle and a monomer in the brush. The radius of the spherical nanoparticle is characterized by $R_0 = 3\sigma_{\mathrm{mm}}$. We choose $\epsilon_{\text{m-np}} = 4$ and $\sigma_{\text{m-np}} = 1$ [27]. Although this choice is not necessarily a realistic one, it is very efficient from a computational point of view.

The motion of the i-th monomer follows the Langevin equation:

$$m\ddot{\boldsymbol{r}}_i = -\frac{\partial U}{\partial \boldsymbol{r}_i} - m\gamma\dot{\boldsymbol{r}}_i + \eta_i(t), \tag{4}$$

where $m = 1$ is the mass of monomer, γ denotes the friction coefficient, and η is a random force modeling the collisions by solvent molecules. $\eta_i(t)$ has zero mean over time and satisfies the fluctuation-dissipation theorem,

$$\langle \eta_i(t)\eta_j(t')\rangle = 6k_{\mathrm{B}}Tm\gamma\delta_{ij}\delta(t-t'). \tag{5}$$

The nanoparticle observes the same Langevin equation with $m_{\mathrm{np}} = 20$ [27], so that we expect to be able to observe Brownian motion of the particle in the brush.

The lateral linear dimensions are L_x and L_y, respectively. Each polymer is grafted at one end randomly onto the lower surface at $z = 0$. Periodic boundary conditions are used in the horizontal planes. We take the number of end-grafted chains to be M, containing N effective monomers each. So the grafting density is $\sigma = M/(L_xL_y)$. For comparison, polymer brushes with different grafting densities have been studied.

The velocity-Verlet scheme [28] is used for integration of the Langevin Eq. (4), with integration time step $\delta t = 0.01\sigma_{\mathrm{mm}}\sqrt{m/\epsilon_{\mathrm{mm}}}$. $\sigma_{\mathrm{mm}}\sqrt{m/\epsilon_{\mathrm{mm}}}$ is the corresponding reduced unit of time. The friction constant in the Langevin equation is $\gamma = 0.5$. In most of the cases, the simulations are carried out until the brush is under equilibrium state, based on the gyration radius of the brush chains. After equilibration of the polymer brush, the nanoparticle is placed onto the top surface of the brush. Then, the particle is embedded into the brush and the system equilibrates after long enough time steps.

3. Results

A representative embedding process of a nanoparticle into brush is shown in Fig. 1, for a polymer brush made of 400 chains of length $N = 40$ in a simulation box $L_x = L_y = 39.0$, which corresponds to grafting density $\sigma = 0.263$. The vertical positions of the nanoparticle, z_{np}, as functions of time are shown in Fig. 2. The z_{np} is averaged from 10 runs like Fig. 2 but with different initial brush equilibrium configurations, and shown in Fig. 3c.

TABLE

Values of the parabolic fit of Eq. (6) for $N = 41$ for different values of σ.

σ	C_1	C_2	$(C_1/C_2)^{1/2}$	h	$\langle z\rangle$	$h/\langle z\rangle$
0.0278	1.385	1.054	1.146	14.2	6.28	2.26
0.148	1.922	1.725	1.055	22.8	9.75	2.33
0.263	2.435	2.268	1.036	27.2	11.92	2.28

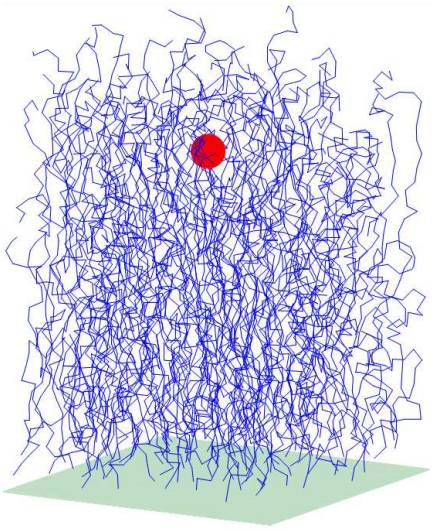

Fig. 1. Snapshot of the embedded nanoparticle in the brush with grafting density $\sigma = 0.263$ and $N = 40$. For clarity, only the nanoparticle and its nearby polymer chains are plotted here. The nanoparticle is schematically denoted as the red solid circle.

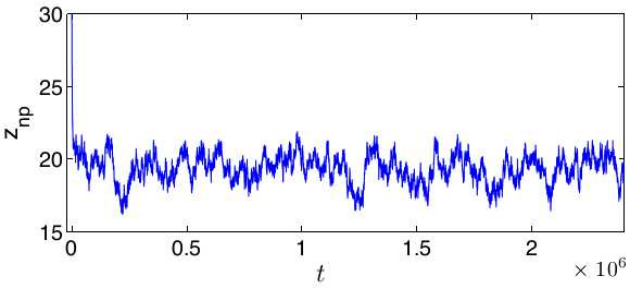

Fig. 2. The vertical position of nanoparticle, z_{np}, as a function of time. Our simulation starts from the state of the nanoparticle placed onto the top of the brush.

Let us now turn to the properties of the brush we obtained. In Fig. 3, the density profiles of the monomers as well as the positions of the nanoparticle are shown as a function of the distance z to the substrate for the low, moderate, and high grafting densities. A depletion region for monomer density is observed due to the hard core of the monomers directly at the substrate. Here, only the sink case for the nanoparticle into the brush is shown. Note that the length of the brush above the nanoparticle (i.e., the part of the brush for $z > z_{\mathrm{np}}$) decreases with the increment of grafting density. It is natural that the nanoparticle will be well localized at the top surface of the brush for a enough dense coverage.

Milner, Witten, and Cates's polymer brush theory showed that the density profile for polymer brushes of short chains could be described with a parabolic equation:[29–31]

$$\rho(z) = \rho_0 - \alpha z^2 \tag{6}$$

with $\rho_0 = C_1\sigma^{2/3}$ and $\alpha = C_2N^{-2}$ (C_1 and C_2 are two adjustable parameters). We also show that the $\rho(z)$

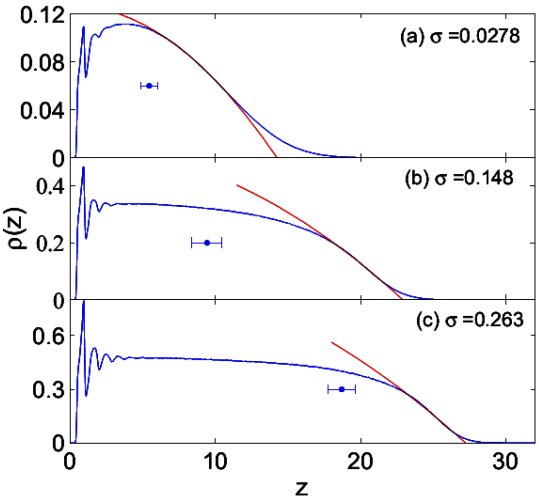

Fig. 3. Monomer number density, $\rho(z)$, as a function of the distance, z, from the grafting surface for chains of length $N = 41$ at different coverages: (a) $\sigma = 0.0278$, (b) $\sigma = 0.148$, (c) $\sigma = 0.263$. The solid circles and the corresponding error bars, which are calculated based on the data like that in Fig. 2, show the positions ($z_{\rm np}$) of the embedded nanoparticle. The red solid lines are the parabolic fits to the form of Eq. (6). The details of the fits are listed in Table.

curves can be well approximated by this parabolic form of Eq. (6) for all values of σ and N in Fig. 3. At low surface density, σ, parabolic function was applicable to a majority of the chain monomers; while, at high surface density, parabolic form was applicable only for the chain end far from the tethering surface [22, 31].

Our values for C_1 and C_2 are shown in Table. From this, we can give the height of the brush,

$$h = \left(\frac{\rho_0}{\alpha}\right)^{1/2}. \tag{7}$$

Expanding h, one gets

$$h = \left(\sigma^{2/3} N^2 \frac{C_1}{C_2}\right)^{1/2} = N\sigma^{1/3}\left(\frac{C_1}{C_2}\right)^{1/2}. \tag{8}$$

From Table, we see $(C_1/C_2)^{1/2}$ trends toward unity. This fits well with the scaling theory of Alexander [32] and the self-consistent field theory of Milner et al. [29, 33], which predict that the height of the polymer brush will grow with the molecular weight and the surface coverage as

$$h \sim N\sigma^{1/3}. \tag{9}$$

We have also calculated $h/\langle z\rangle$, where $\langle z\rangle$ is the average thickness of the brush defined by

$$\langle z\rangle = \frac{\int z\rho(z)\,{\rm d}z}{\int \rho(z)\,{\rm d}z}. \tag{10}$$

We see that $h \approx 2.3\langle z\rangle$ for all cases. This is in good agreement with the data in Ref. [22].

We also measured the lateral diffusion coefficient of nanoparticle as a function of the penetration depth z in Fig. 4. For the interested lateral motion of particle,

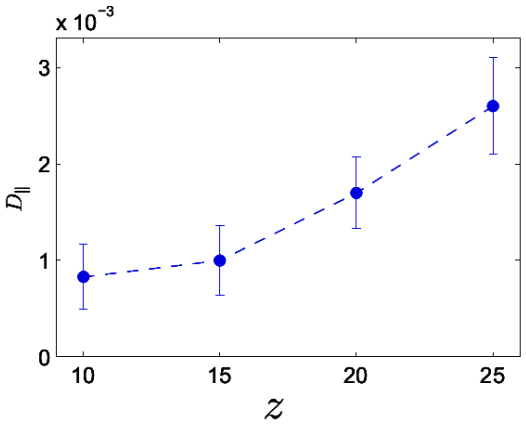

Fig. 4. The lateral diffusion coefficient $D_\parallel$, as a function of the distance, z, from the grafting surface for nanoparticle with $R = 3$ and brush with chains of length $N = 50$ at $\sigma = 0.205$.

a potential is applied to allow the particle's motion only in the lateral plane,

$$U = U_0(z - z_0)^2, \tag{11}$$

where z_0 is the target depth of the particle, and U_0 is a potential constant which is large enough to confine the particle motion in the lateral plane.

The calculations were performed taking $\epsilon_{\text{m-np}} = 2$. For each value of z_0, the system runs for 10^6 MD steps, and then six successive runs of 10^6 MD steps were performed, where each run started with the final configuration of the previous one. The diffusion coefficient was determined for each of the six runs and then averaged. The diffusion coefficient $D_\parallel$, for lateral diffusion parallel to the substrate, is defined via [34]:

$$D_\parallel = \lim_{t\to\infty} \frac{\left[\boldsymbol{r}_\parallel(t) - \boldsymbol{r}_\parallel(0)\right]^2}{6Nt}, \tag{12}$$

where $\boldsymbol{r}_\parallel$ is the projection of the position vector of the nanoparticle. As shown in Fig. 4, it is obvious that increasing the depth z of the particle, decreases the diffusion of particle in the brush. Let us note that the diffusion coefficient is of the order of 10^{-3}, which implies that the dimensionful coefficient is of the order of 10^{-6} cm^2/s [34].

In experiment related to the adsorption of nanocolloidal SiO_2 particles onto brushes, there is a maximum in the adsorbed amount as a function of the grafting density [19]. To a certain extent, from the degree of one nanoparticle penetration in polymer brush, one can qualitatively analyze the absorbed amount of many nanoparticles on brush in experiments. It can be seen from the area density of monomer number, Γ, which is the surface average of the sum of all the monomers above the nanoparticle,

$$\Gamma = \sum_i^{MN} \delta(z_i > z_{\rm np})/(L_x L_y). \tag{13}$$

Figure 5 shows the area density, Γ, as a function of the

grafting density, σ. It exhibits a maximum, which means the maximal number of adsorption sites per area for the nanoparticles. Clearly, from the single nanoparticle point of view, the adsorbed amount of nanocolloids on brush is determined by the coupling of the grafting density and the penetration depth of the particle. If the grafting density increases, the number of the monomers absorbing nanoparticles should increase correspondingly. However, the dense chains will exclude the particle from the inner part of the brush due to the strong steric interactions. This results in a small penetration depth, hence, a small amount of adsorption monomers above the embedded nanoparticle. Otherwise, a deep penetration of the particle requires a loose grafting density, which will decrease the amount of absorbing monomers. Therefore, the combination of increasing grafting density and decreasing penetration depth results in a maximum in the adsorption amount of monomers, as illustrated in Fig. 5, which predicts a behavior qualitatively similar to that in Ref. [19].

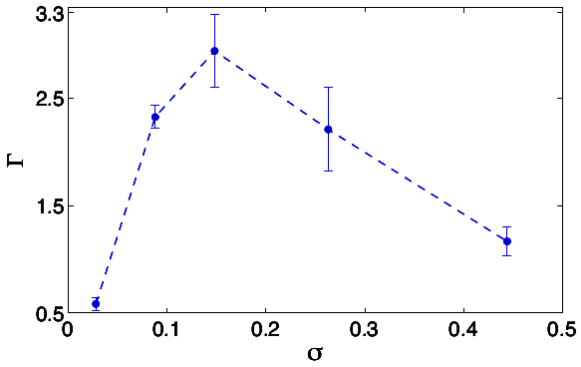

Fig. 5. The area density, Γ, of the brush monomers above the embedded nanoparticle, as a function of the grafting density, σ. From left to right, the 5 solid circles correspond to $\sigma = 0.0278, 0.0878, 0.148, 0.263, 0.444$, respectively. The dotted line is just a guide to the eye.

Let us note that in Fig. 5, the error bars are larger for the moderate grafting density ($\sigma = 0.148,\ 0.263$) than that for the low grafting density ($\sigma = 0.278,\ 0.0878$) and the high grafting density ($\sigma = 0.444$). The reasons are analyzed as follows. For loose polymer chains, it is mainly the adsorption interaction between monomers and nanoparticle plays a role in absorbing and hindering the nanoparticle's free movement. While for dense brush, it is mainly the steric repulsion between monomers and nanoparticle that obstructs the nanoparticle's motion. In moderate grafting density, the combination of the adsorption and steric repulsion between monomers and nanoparticle causes the nanoparticle to move more freely than it does in the low and the high grafting densities.

It should be stressed that it is the area density not the bulk density of monomers above the embedded nanoparticle, that qualitatively explains the maximal adsorption amount of nanocolloids on brush with different coverages. It is obvious that the bulk density of monomers of the dense brush (for example $\sigma = 0.444$) is larger than that of the loose brush (for example $\sigma = 0.148$). But, the adsorption amount of monomers per area (i.e., Γ) of the former is smaller than that of the latter, as shown in Fig. 5. What absorbs the nanoparticles is all the polymer monomers above the embedded particle, not the monomers in a unit volume only.

We hope that the area density Γ is helpful for the analysis of the absorbed amount of nanoparticles on brush in Ref. [19]. In fact, we simply use the sum of all the monomers above the nanoparticle to analyze the overall adsorbed amount of nanoparticles. Although these two quantities exhibit the same qualitative behavior, the following effects should not be ignored in the analysis: the effects between nanoparticle interactions; the effects of individual nanoparticle on the chain configuration of polymer brush, such as the squeezed polymer chains under the particle. These effects should certainly influence the adsorption process.

4. Conclusions

We have reported on Brownian dynamics simulation results of the embedding process of a nanoparticle into a polymer brush. The brush density has been compared to and well fitted by the Milner, Witten, and Catess polymer brush theory. A detailed discussion of the adsorption process, the penetration depth, and the dynamic behavior of nanoparticle in brush have been explored. For an interesting phenomenon in experiment that the absorbed amount of nanocolloids on brush behaves a maximum as functions of grafting density, we give a detailed qualitative explanation, based on the model in the present paper of single nanoparticle adsorption on brush, by using the area density of monomers above the embedded particle. It should be interesting to examine the influences of other parameters on the adsorption process, for example, the electrostatic interactions between the nanoparticle and the brush. Other parameters that may be considered are the chain length, the polydispersity, the size of particle, and the adsorption strength between particle and polymer monomers.

Acknowledgments

This research is funded by the National Natural Science Foundation of China (grant No. 20804060).

References

[1] Z. Liu, K. Pappacena, J. Cerise, J. Kim, C.J. Durning, B. O'Shaughnessy, R. Levicky, *Nano Lett.* **2**, 219 (2002).

[2] R.R. Bhat, J. Genzer, B.N. Chaney, H.W. Sugg, A.L. Vinson, *Nanotechnology* **14**, 1145 (2003).

[3] I. Tokareva, S. Minko, J.H. Fendler, E. Hutter, *J. Am. Chem. Soc.* **126**, 15950 (2004).

[4] E. Filippidi, V. Michailidou, B. Loppinet, J. Ruhe, G. Fytas, *Langmuir* **23**, 5139 (2007).

[5] J.U. Kim, M.W. Matsen, *Macromolecules* **41**, 246 (2008).

[6] O.A. Guskova, S. Pal, C. Seidel, *Europhys. Lett.* **88**, 38006 (2009).

[7] A. Milchev, D.I. Dimitrov, K. Binder, *Polymer* **49**, 3611 (2008).

[8] A. Elgsaeter, B.T. Stokke, A. Mikkelsen, D. Branton, *Science* **234**, 1217 (1986).

[9] D.H. Napper, *Polymeric Stabilization of Colloidal Dispersions*, Academic Press, London 1983.

[10] R.B. Thompson, V.V. Ginzburg, M.W. Matsen, A.C. Balazs, *Science* **292**, 2469 (2001).

[11] V.Z.-H. Chan, J. Hoffman, V.Y. Lee, H. Iatrou, A. Avgeropoulos, N. Hadjichristidis, R.D. Miller, E.L. Thomas, *Science* **286**, 1716 (1999).

[12] M. Cohen, D. Joester, B. Geiger, L. Addadi, *Chem. Bio. Chem.* **5**, 1393 (2004).

[13] M. Cohen, E. Klein, B. Geiger, L. Addadi, *Biophys. J.* **85**, 1996 (2003).

[14] E. Zimmerman, B. Geiger, L. Addadi, *Biophys. J.* **82**, 1848 (2002).

[15] S.T. Milner, *Science* **251**, 905 (1991).

[16] J. Kaldasch, B. Senge, *Colloid Polym. Sci.* **287**, 1481 (2009).

[17] T. Drobek, N.D. Spencer, M. Heuberger, *Macromolecules* **38**, 5254 (2005).

[18] S.R. Sheth, D. Leckband, *Proc. Natl. Acad. Sci. U.S.A.* **94**, 8399 (1997).

[19] R.A. Gage, E.P.K. Currie, M.A.C. Stuart, *Macromolecules* **34**, 5078 (2001).

[20] Q.Y. Zhang, K.R. Li, H.Y. Tang, *Int. J. Mod. Phys. B* **25**, 1899 (2011).

[21] Q.Y. Zhang, X. Xiang, K.Y. Hu, *Mod. Phys. Lett. B* **26**, 1250089 (2012).

[22] M. Murat, G.S. Grest, *Macromolecules* **22**, 4054 (1989).

[23] D. Bedrov, G.D. Smith, *Langmuir* **22**, 6189 (2006).

[24] K. Kremer, G. Grest, *J. Chem. Phys.* **92**, 5057 (1990).

[25] G.S. Grest, K. Kremer, *Phys. Rev. A* **33**, 3628 (1986).

[26] D.I. Dimitrov, A. Milchev, K. Binder, *J. Chem. Phys.* **127**, 084905 (2007).

[27] J.G.D. Ochoa, K. Binder, W. Paul, *J. Phys., Condens. Matter* **18**, 2777 (2006).

[28] M.P. Allen, D.J. Tildesley, *Computer Simulation of Liquids*, Clarendon, Oxford 1987.

[29] S.T. Milner, T.A. Witten, M.E. Cates, *Macromolecules* **21**, 2610 (1988).

[30] A. Chakrabarti, R. Toralt, *Macromolecules* **23**, 2016 (1990).

[31] L.A. Strickland, C.K. Hall, J. Genzer, *Macromolecules* **41**, 6573 (2008).

[32] S. Alexander, *J. Phys. (Paris)* **38**, 983 (1977).

[33] S.T. Milner, T.A. Witten, M.E. Cam, *Europhys. Lett.* **5**, 413 (1988).

[34] A. Imparato, J.C. Shillcock, R. Lipowsky, *Eur. Phys. J. E* **11**, 21 (2003).